

# Early Detection of Defects in Gear Systems Using Autocorrelation of Morlet Wavelet Transforms

Mouloud Ayad<sup>1,2</sup> – Kamel Saoudi<sup>1,2</sup> – Mohamed Rezki<sup>1</sup> – Mourad Benziane<sup>1,2</sup> – Abderrazak Arabi<sup>3</sup>

<sup>1</sup>University of Bouira, Faculty of Sciences and Applied Sciences, Department of Electrical Engineering, Algeria

<sup>2</sup> University of Bouira, LPM3E Laboratory, Algeria

<sup>3</sup> University of Sétif 1, LIS Laboratory, Algeria

*The supervision task of industrial systems is vital, and the prediction of damage avoids many problems. If any system defects are not detected in the early stage, this system will continue to degrade, which may cause serious economic loss. In industrial systems, the defects change the behaviour and characteristics of the vibration signal. This change is the signature of the presence of the defect. The challenge is the early detection of this signature. The difficulty of the vibration signal is that the signal is very noisy, non-stationary and non-linear. In this study, a new method for the early defect detection of a gear system is proposed. This approach is based on vibration analysis by finding the defect's signature in the vibration signal. This approach has used the autocorrelation of Morlet wavelet transforms (AMWT). Firstly, simulation validation is introduced. The validation of the approach on a real system is given in the second validation part.*

**Keywords:** Autocorrelation of Morlet Wavelet Transforms, early fault diagnosis, gear systems, Vibration analysis, Scalograms

## Highlights

- A new approach for early defect detection of a gear system is proposed.
- The autocorrelation of Morlet wavelet transforms (AMWT) is used to detect the presence of faults.
- The study is based on both simulation and experimental validation.
- This approach helps the professionals in the supervision of mechanical systems.

## 0 INTRODUCTION

Supervision of industrial systems is an essential task to guarantee performance and reliability. The crucial key of this supervision is understanding the equipment behaviour, and the information extracted can be used for planning maintenance activities. Therefore, the monitoring aims to increase profitability by reducing downtime and increasing the lifetime of the equipment. Consequently, the early detection of defects in mechanical systems is essential for operators and has attracted the attention of many researchers in recent years [1] to [6]. They aim to plan to repair these systems rather than catastrophic damage caused by unexpected defects. The most well-known techniques for the prevention of rotating systems are temperature control (thermography) [7] and [8], oil debris control [9] and [10], acoustic analysis [11] and [12] and vibration signal control (analysis) [13] and [14]. The significant advantage of vibration analysis is that it can detect and identify the defect evolution before it becomes severe and causes catastrophic damage. This can be accomplished by the regular monitoring of the vibration machine. Therefore, the monitoring aim is to increase productivity by reducing downtime and increasing the lifetime of the equipment.

There are several techniques in the literature proposed for early fault detection based on vibration analysis. In general, there are three domains of vibration signal processing for defect diagnosis of rotating machines: time domain, frequency domain, and time-frequency domain. The basic principle of vibration analysis is based on the fact that a change in the mechanical system's conditions can induce a change in the vibrations produced by this system. In simple systems, this change can affect the shape by an increase in the amplitude of the signal. For complex systems, the detection of change in the vibration signal, affected by the deterioration of the system, is very complicated and more sophisticated techniques of detection are required.

A gear system is an essential element usually used in a range of industrial systems. Therefore, accurate and early defect detection and correct diagnoses are vital to normal machinery operations. When a localized defect occurs in gears, the characteristics of periodic impulsive of the signal appear in the time domain, and the corresponding frequency components will be affected. However, an effective signal analysis approach is needed to eliminate noise and interference. In the literature, several approaches are proposed. For example, Matic and Kanovic [13] used the vibration signal analysis based on current signal

analysis by observing fault frequency content to detect a broken bar fault. In [14], a reassigned short-time Fourier transform (RSTFT) is presented to identify the sideband components related to the failure of the broken rotor bar in the induction motors. Wang et al. [15] propose an adaptive parameter identification method for gearbox defect detection. It combines the Morlet wavelet and the correlation filtration for characterizing both the cyclic period between adjacent impulses and the impulse response.

In this work, we propose a new approach based on the autocorrelation function of Morlet wavelet transforms. This approach is applied firstly on simulated signals, and secondly on real gear signals for the early detection of defects present in an experimental tested gear system.

The remainder of this present work is planned as follows: in Section 2, the theoretical background of AMWT is given. Next, the simulation validation is introduced in Section 3. In Section 4, the obtained results and the validation of the approach on a real system are given.

## 1 THEORETICAL BACKGROUND

In this section, we explain the approach proposed for the fault diagnosis of a gear system. This approach is based on the autocorrelation of Morlet wavelet transforms (AMWT). Therefore, we give the background of the Morlet wavelet transform (MWT) and then the autocorrelation of Morlet wavelet transform (AMWT).

### 1.1 Morlet Wavelet Transform

The wavelet transform can address the problem of temporal and frequency resolution through multi-resolution analysis. As the name signifies, multi-resolution analysis allows for different temporal and frequency resolutions. It provides an excellent frequency resolution (i.e., poor temporal resolution) at low frequencies and an excellent temporal resolution (i.e., a poor frequency resolution) at high frequencies. This analytical approach is particularly advantageous for signals with low-frequency components for an extremely short period and high-frequency components for relatively extended periods. For the non-stationary signals analysis, the wavelet transform is adequate because it provides a simultaneous localization of time and frequency.

For any signal  $x(t)$ , the continuous wavelet transform (CWT) is given by:

$$\text{CWT}_{x(t)} = |a|^{-1/2} \int_{-\infty}^{+\infty} x(t) \Psi^* \left( \frac{t-b}{a} \right) dt, \quad (1)$$

where  $*$  is the symbol of a complex conjugate function;  $a$  the parameter of dilation,  $b$  the parameter of translation, and  $\Psi$  represent the mother wavelet represented by [15]:

$$\Psi_{a,b}(t) = |a|^{-1/2} \Psi \left( \frac{t-b}{a} \right). \quad (2)$$

The translation parameter controls the shifting position, and the dilation parameter controls the oscillation frequency [16] and [17].

The wavelet of Morlet represents functions with the form of small waves created by dilations and translations from the mother wavelet given by [4]:

$$\Psi(t) = \exp(j2\pi f_c t) \exp(-t^2 / f_b), \quad (3)$$

where  $f_b$  is the parameter of bandwidth, and  $f_c$  the central frequency of the wavelet.

These two parameters control the form of the Morlet wavelet.

After calculating the CWT, we calculate the scalogram defined as the square of the CWT module.

### 1.2 Autocorrelation of Morlet Wavelet Transform

Random vibrations are inherently unpredictable, so the future values of the signal can be defined only based on probabilities. We consider the random signal to be the stochastic process realization, i.e., the time evolution of a random variable. We speak about the cyclostationnarity of a stochastic process representing the signal when the government's statistical parameters that govern vary periodically. The autocorrelation function calculates the internal dependencies of the signal. For example, in the case of the sinusoidal signal, the autocorrelation coefficients are highly uniform and homogeneous; therefore, the signal will have a strong autocorrelation. The rotating machine's vibration signals consist of periodic and random components.

The autocorrelation function  $R_x(t)$  of a signal  $x(t)$ , is usually the cross-correlation of the signal  $x(t)$  with itself. The cross-correlation of a signal  $x(t)$  and  $y(t)$  is given by the expression [18] and [19]:

$$R_{xy}(t) = \sum_{n=0}^{\infty} x(n)y(n+r), \quad (4)$$

where  $r$  is a time step.

If  $x(n) = y(n)$ , the Eq. (4) becomes an autocorrelation function:

$$R_x(t) = E[x(t), x(t-\tau)], \quad (5)$$

where  $\tau$  is the specific time step (lag).  $E [ , ]$  is the expectation or averaging operator.

The autocorrelation of an ergodic process is defined by:

$$R_x(t) = \lim_{T \rightarrow \infty} \frac{1}{T} \int_0^T x(t)x(t+\tau)dt. \quad (6)$$

The autocorrelation attains its peak in the beginning:

$$|R_x(\tau)| \leq |R_x(0)|. \quad (7)$$

The autocorrelation of the wavelet coefficients is the integral of the product of the wavelet transform  $WT_{a,b}(t)$  with itself delayed by  $(\tau)$  according to the following equation:

$$R_{xx}(t) = \int_{-\infty}^{+\infty} WT_{a,b}(t) \times WT_{a,b}(t+\tau)dt. \quad (8)$$

The autocorrelation function reaches its maximum peak at the centre. We call this centre point a maximum peak point (MPP). Suppose the size of a function  $x(t)$  is equal to  $M$  where  $M > 1$ , the autocorrelation function has a dimension of  $2 \times (M-1)$ . The proposed method for predicting defects of rotating machines consists of calculating the autocorrelation of the Morlet wavelet transform (MWT). In this case, the MWT is a two-dimensional matrix ( $M \times N$ ), and in consequence, the autocorrelation function will also be two dimensional ( $\mathbf{O} \times \mathbf{P}$ ) with  $\mathbf{O} = 2 \times (M-1)$  and  $\mathbf{P} = 2 \times N-1$ .

## 2 SIMULATION EVALUATION

In this part, the performance of the proposed approach is examined on simulated signals. The vibration signals measured in the gear systems are very complicated and have multi-components: tooth vibration, vibration of gear shaft rotation, gear resonance vibration and vibration due to various gearing defects. To simulate these various vibration components and evaluate the performance and efficiency of the method, we have used the test signals available in the scientific literature. It is noted here that the autocorrelation function is expressed in three dimensions. To make it possible to estimate the values of the autocorrelation function, we have given another visualization based on the contour of the autocorrelation.

### 2.1 Amplitude and Frequency Modulation

The change in the mechanical conditions of a gear system can produce changes in generated vibration

signal [20]. These changes can take the form of an increase in amplitude or frequency, which will lead to amplitude or frequency modulation. In general, frequency modulation is significantly less significant than amplitude modulation [21].

The following equation gives the test signal modulated in frequency and amplitude:

$$s(t) = [1 + 0.5 \times \sin(6 \times \pi \times t)] \times \sin(100 \times \pi \times t^2). \quad (9)$$

The temporal representations of the signal modulated in frequency and amplitude of Eq. (9) and its MWT scalograms and AMWT autocorrelation are given in Fig. 1.

The scalograms of this signal (Fig. 1a) demonstrate the presence of amplitude and frequency modulation. We observe this modulation: the amplitude modulation results in the amplitude variations of the coefficients and the frequency modulation by their non-linear localisation. The representation of the autocorrelation of a signal modulated in frequency and amplitude is given in Figs. 1c and d. In this case, the MPP point has an amplitude of  $MPP(1000, 25) = 1.1369177 \times 10^6$ .

### 2.2 Simulation of the Gear Vibration Signal

In real systems, to facilitate diagnostic and predictive techniques for gear systems, it is necessary to simulate models in which defects can be implemented under different operating conditions instead of waiting for the natural occurrence of these defects. Many models of meshing signals have been proposed in the literature [18] and [20] to [22]. In our case, we will use two models of the gear signal; it is the gear vibration signal simulated by McFadden [20] and the one introduced by Qin et al. [22]. The first model proposed in the literature is that of McFadden [20]. This model is also used by several researchers: Yin et al. [21], Man et al. [23] and others.

### 2.3 Case Study 1: Gear Simulated by Qin

For rotating machines, the measured signal is the sum of the components of the signal generated by the different mechanisms of the machines. The monitoring of the machine is allowed by the analysis of the vibration signal. However, the essential defect characteristics are incorporated into the components of the signal. In several cases, obtaining the defect information directly from the original signal is a challenging task. Therefore, the useful components must be separated from the measured signal. The

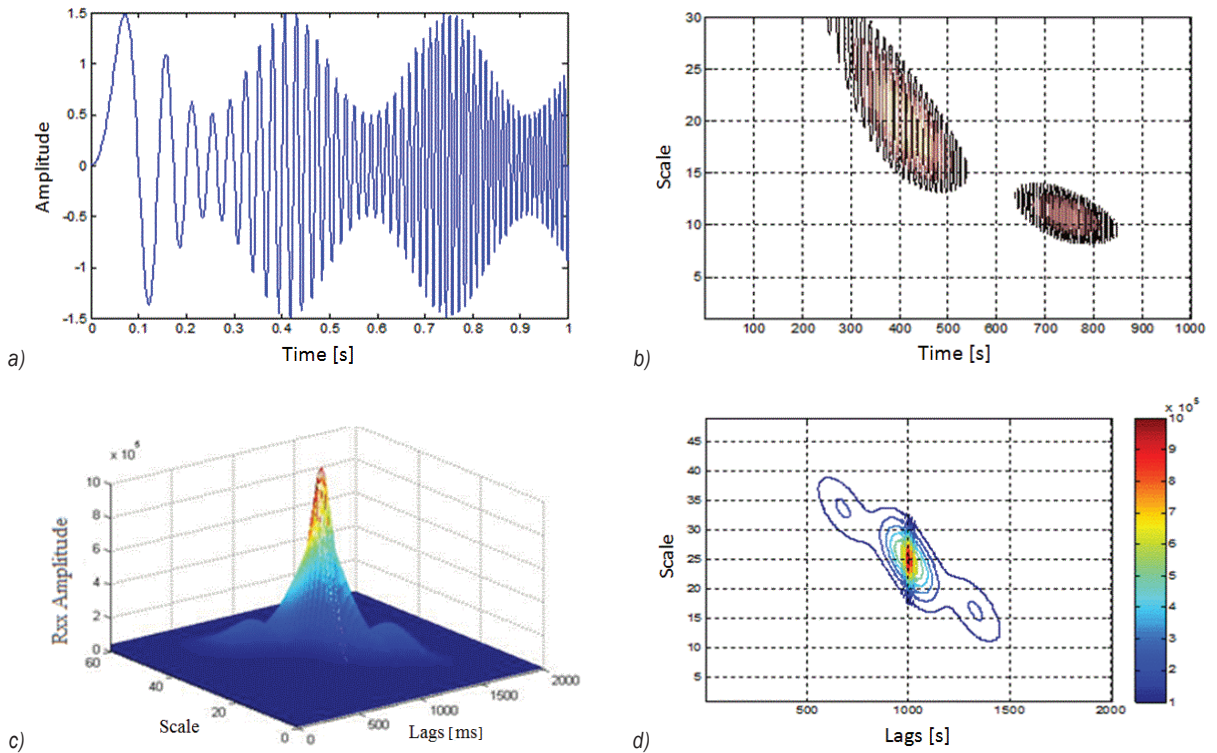


**Fig. 1.** Signal modulated in amplitude and frequency; a) temporal representation, b) MWT scalograms, c) AMWT autocorrelation, and d) contour of AMWT autocorrelation

components of the signal are pulses, harmonics and modulated components [22].

In local defects, for example, crack, tooth break, etc., the impulsive force of gear meshing generates a variation in amplitude and the phase of the vibration signal. These variations generate amplitude and phase modulation. In this case, the spectrum analysis of the envelope is an efficient approach for extracting defect information. The gear vibration signal simulated by Qin et al. [22] is given by  $x(t)$  :

$$x(t) = x_1(t) + x_2(t) + x_3(t), \quad (10)$$

with:

$$x_1(t) = [0.4 + 0.4 \sin(2\pi \times 10t)] \times \cos[2\pi \times 700t + 1.5 \sin(2\pi \times 10t)], \quad (11)$$

$$x_2(t) = [1 + \sin(2\pi \times 5t)] \times \cos[2\pi \times 350t + \sin(2\pi \times 5t)], \quad (12)$$

$$x_3(t) = [0.6 + 0.6 \cos(2\pi \times 5t)] \times \cos[2\pi \times 200t + 0.6 \sin(2\pi \times 5t)]. \quad (13)$$

The sampling frequency is 3 kHz. In general, the gear vibration signal is always accompanied by noise.

Hence studying the simulated gear vibration signal with noise is necessary. To this end, we added white noise to the gear vibration signal of Qin et al. [22]. Fig. 2a shows the temporal representation of the defective gear signal simulated by Qin et al. [22], with noise.

In the case in which the signal is embedded in the noise, the effect of the modulation is present on the scalograms. We observe an amplitude peak at the MPP point equal to  $MPP(1000, 30) = 6.27234110 \times 10^7$ .

#### 2.4 Case study 2: Gear Defects Simulated by McFadden

The meshing vibration signal is periodic and simultaneously modulated in frequency and amplitude by a periodic signal equal to the period of gear meshing. In general, amplitude modulation is more critical than frequency modulation [21].

Consider a pair of gears that mesh with constant load and speed, with several different teeth. Thus, the vibration signal  $x(t)$  of meshing without defect is given by [20]:

$$x(t) = \sum_{m=0}^M X_m \cos(2\pi \cdot m \cdot Z \cdot f_r \cdot t + \phi_m), \quad (14)$$

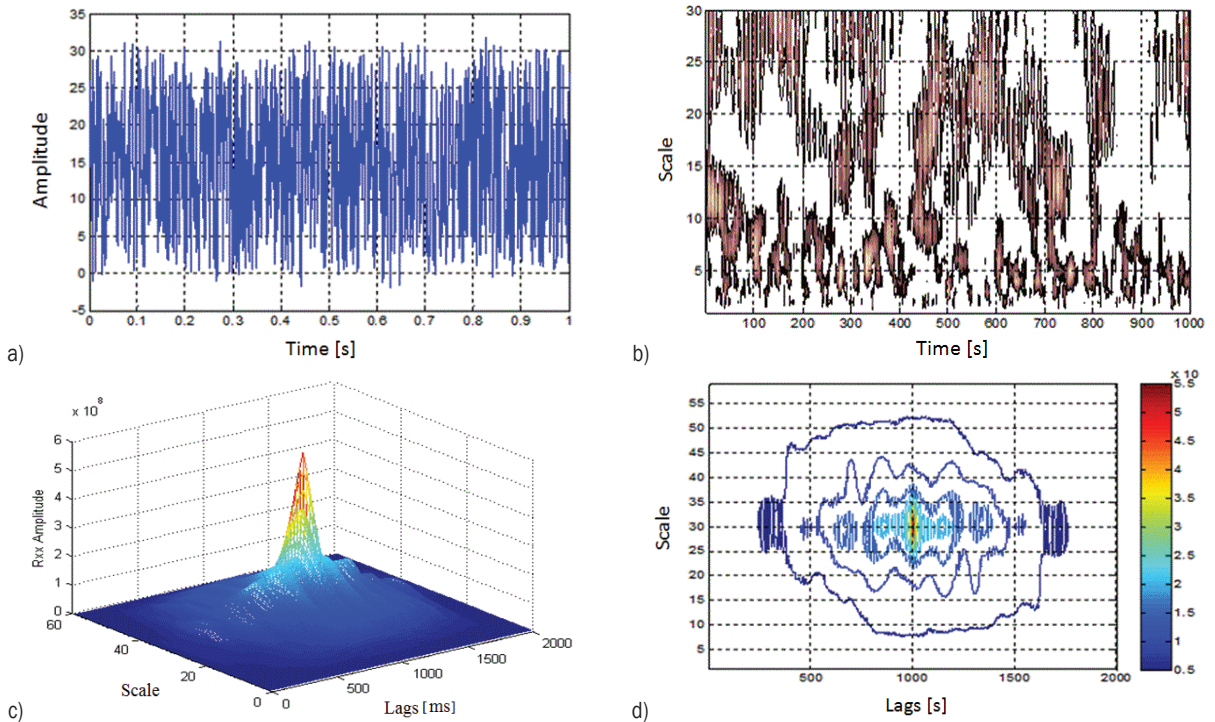


**Fig. 2.** Gear vibration signal of Qin; a) temporal representation, b) MWT scalograms, c) AMWT autocorrelation and d) contour of AMWT autocorrelation

where  $M$  is the range of analysis,  $X_m$  the amplitude of the harmonic [m],  $Z$  the number of teeth,  $f_r$  the rotation frequency of the tree, and  $\phi_m$  the phase.

If the gear has a fault (crack, for example), this will affect the meshing signal's phase and amplitude modulation. The modulated signal is given [20], [21] and [23] by:

$$y(t) = \sum_{m=0}^M X_m [1 + a_m(t)] \times \cos[2 \cdot \pi \cdot m \cdot Z \cdot f_r \cdot t + \phi_m + b_m(t)], \quad (15)$$

where

$$a_m(t) = \sum_{n=0}^p A_{mn} \cos(2 \cdot \pi \cdot m \cdot f_r \cdot t + \alpha_{mn}), \quad (16)$$

$$b_m(t) = \sum_{n=0}^p B_{mn} \cos(2 \cdot \pi \cdot m \cdot f_r \cdot t + \beta_{mn}). \quad (17)$$

$a_m(t)$  and  $b_m(t)$  are respectively the functions of amplitude and frequency modulations of the meshing signal caused by the tooth defect.

$\alpha_{mn}$  and  $\beta_{mn}$  are respectively the phases of  $a_m(t)$  and  $b_m(t)$ .

To give this study a near meaning to the real signals, we used the cinematic characteristics of

the Centre d'Etudes Techniques des Industries Mécaniques (CETIM) test bench.

Fig. 3 shows the defective gear vibration signal of McFadden with white noise.

The concentration of the scalogram coefficients of the MWT (Fig. 3b) at the moments when the amplitude peaks are at the maximum is the signature of the presence of the defects.

The representation of the autocorrelation of a signal modulated in amplitude is given in Figs. 3c and d.

We observe a set of amplitude peaks and a maximum peak at the MPP point of amplitude equal to  $MPP(4000, 30) = 4.959990453486705 \times 10^{19}$ .

### 3 RESULTS AND DISCUSSION

To evaluate the efficacy of AMWT, we have examined the proposed method on accurate signals carried out in CETIM [4], [21] and [25]. The system under study is a gear of two wheels (of 20 and 21 teeth). The system operates for 11 days under identical conditions. Every day, the system was examined, and a report about the state of the gear system was delivered.

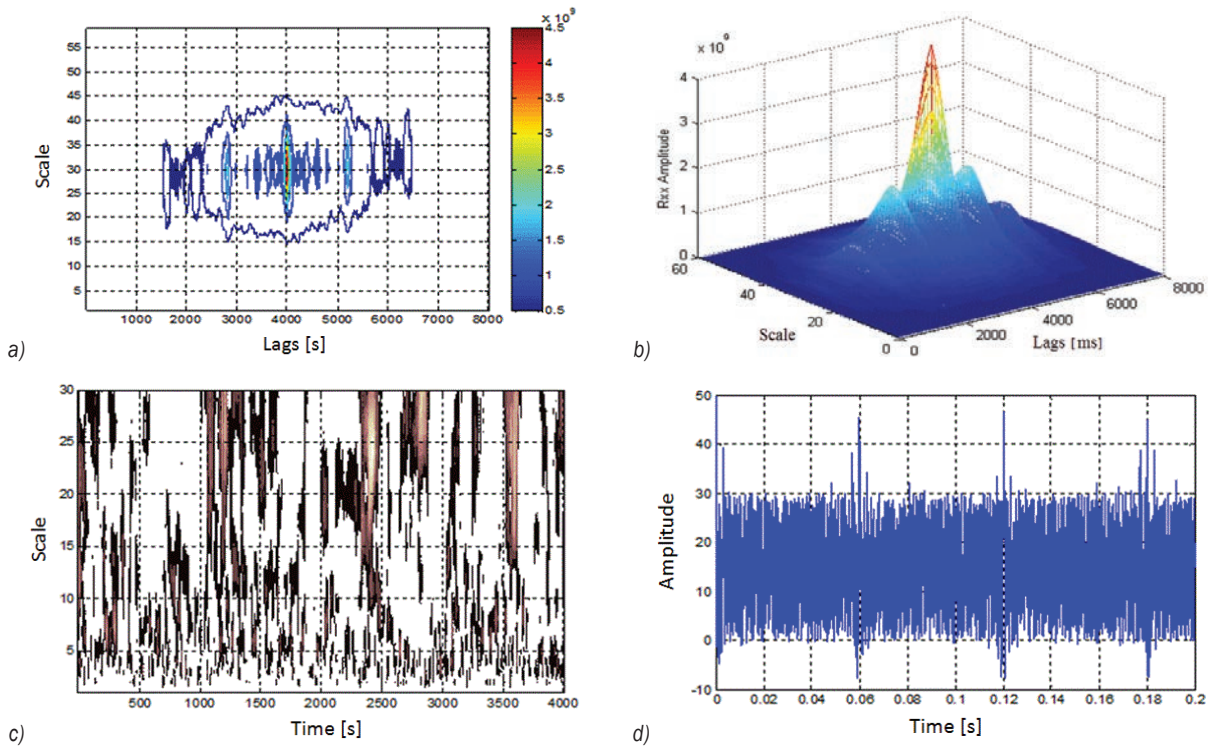


**Fig. 3.** Defective gear vibration signal of McFadden; a) temporal representation, b) MWT scalograms, c) AMWT autocorrelation, and d) contour of AMWT autocorrelation

The studied mechanical system is given in Fig. 4. The expertise report of the experimental system is given in Table 1.

**Table 1.** The expertise report of the experimental system [25]

Day	Observations
1	No anomaly (beginning of the acquisition)
2	No anomaly
3	// //
4	// //
5	Crack of tooth N° (1/2)
6	No evolution
7	Tooth N° (1/2) no evolution, tooth N° (15/16) start of crack
8	Evolution of crack in the tooth N° (15/16)
9	// //
10	// //
11	Crack in all width of the tooth N° (15/16)
12	No anomaly (beginning of the acquisition)

### 3.1 Temporal and Frequency Spectrums

The representations of the temporal vibration signals of the gear system are given in Figs. 4a, b, c and d. We have given the temporal representation of the days: 9, 10, 11 and 12, i.e., one day before the appearance of

the defect and two days after, we arrive to detect the defect on the 10<sup>th</sup> day.

From Figs. 4a, b, c and d, we observe that the temporal representations of vibratory signals  $x(t)$  are approximately similar from the 1<sup>st</sup> until the 11<sup>th</sup> day. However, on the 12<sup>th</sup> day, the behaviour of vibratory signal  $x(t)$  is changed, which is translated by a defect of the tooth deterioration (expertise report in Table 1). The change in the behaviour of the signal vibratory in temporal representation is an indication of the presence of the defect. In consequence, the temporal representation does not detect the presence of the defect early stage.

To prove the method's advantages, we have introduced the fast Fourier transform (FFT) as a comparative study.

The corresponding frequency spectrums of the vibratory signals are shown in Figs. 4a', b', c' and d'.

The side lines are very important on the 12<sup>th</sup> day compared to other days, and this increase is due to the presence of a defect due to the deterioration of a tooth. Thus, the temporal and frequency representation make it possible to diagnose a defect on the last day (12<sup>th</sup> day) and not in the early stage why the necessity of another approach for the early detection.

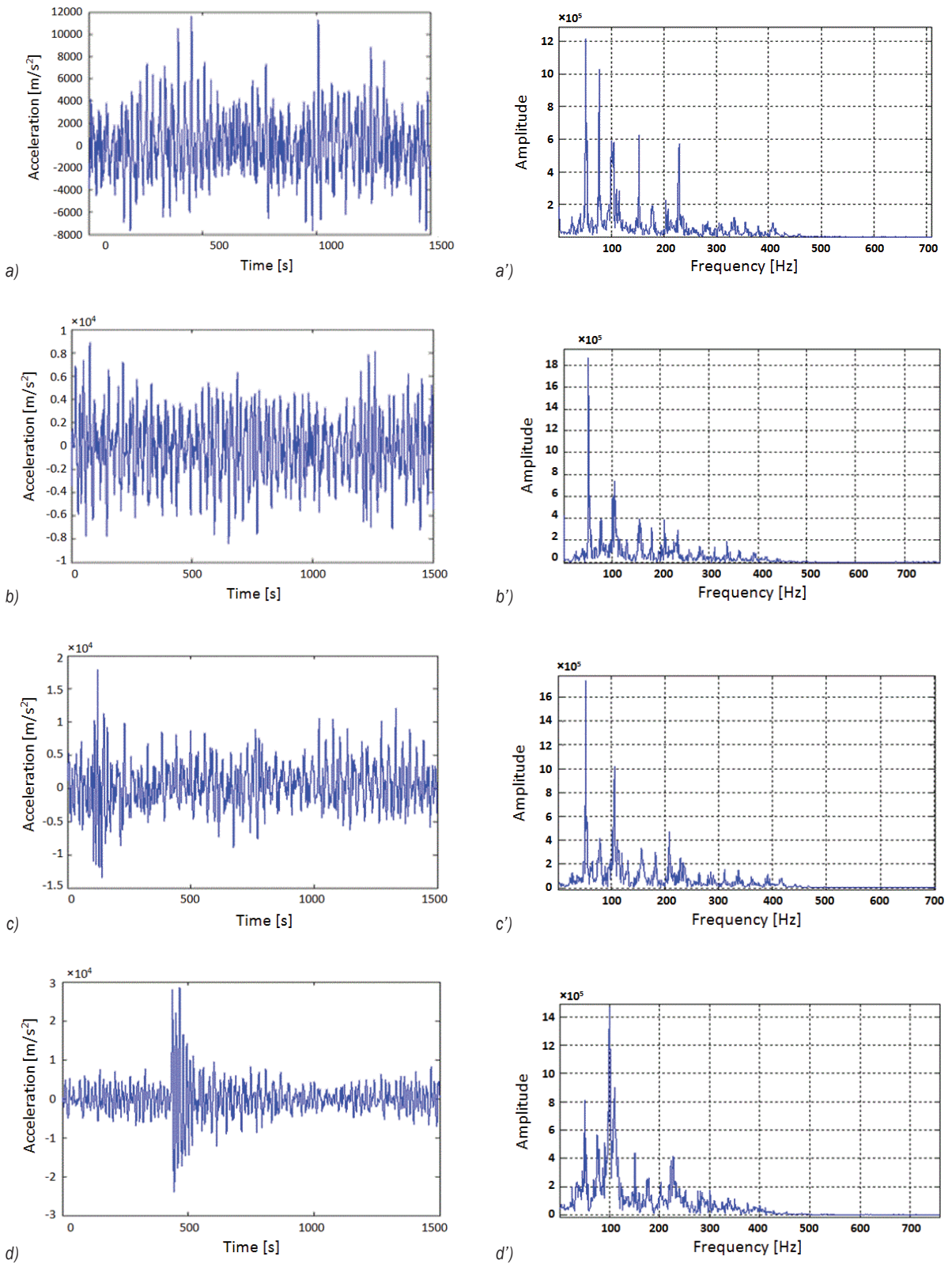


**Fig. 4.** Vibration signals and corresponding frequency spectrums of CETIM gear vibration signal; a, a') 9<sup>th</sup> day, b, b') 10<sup>th</sup> day, c, c') 11<sup>th</sup> day, and d, d') 12<sup>th</sup> day

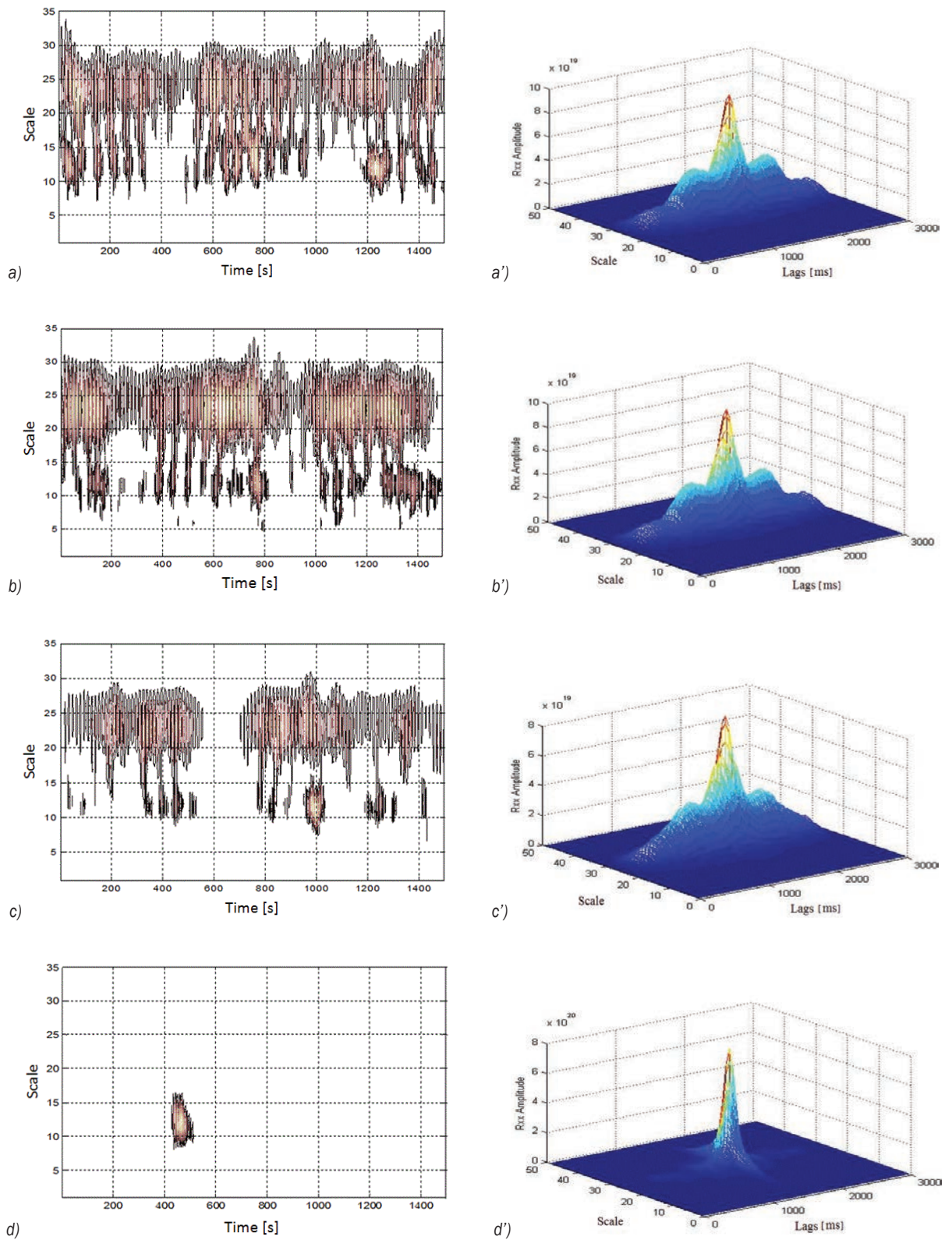


**Fig. 5.** Scalograms and corresponding AMWT of CETIM gear vibration signal; a, a') 9<sup>th</sup> day; b, b') 10<sup>th</sup> day; c, c') 11<sup>th</sup> day, and d, d') 12<sup>th</sup> day



### 3.2 Scalograms Representations and the Autocorrelation of the AMWT

In this part, we apply the approach of the autocorrelation function on scalograms obtained by applying the MWT on vibration signal issued from the CETIM gearbox. The representations of the scalograms and the corresponding AMWT are given in Fig. 5.

From Fig. 6, we observe that the AMWT functions have a similar variation and have the same array of magnitude from the 1st day until the 9th day with the MPP peak amplitude of  $MPP(1500, 25) \approx 6 \times 10^{19}$  (Table 2). These minor changes are caused by several of phenomena, as presented in Table 1.

The MPP peak amplitude values of all days are given in Table 2.

The MPP peak amplitude values of Table 2 are obtained from Fig. 5. They are the maximum peak at the centre.

**Table 2.** The MPP peak amplitude values

Day	MPP peak amplitude
5	$(1500, 25) = 6.626733030945805 \times 10^{19}$
6	$(1500, 25) = 6.090234832595839 \times 10^{19}$
7	$(1500, 25) = 6.586669410632360 \times 10^{19}$
8	$(1500, 25) = 6.437468137514745 \times 10^{19}$
9	$(1500, 25) = 5.090191841432165 \times 10^{19}$
10	$(1500, 25) = 10.04842673892965 \times 10^{19}$
11	$(1500, 25) = 9.084636336550063 \times 10^{19}$
12	$(1500, 25) = 80.54631341778420 \times 10^{19}$

On the 10th day, the autocorrelation function is increased with an MPP peak amplitude of value  $MPP(1500, 25) = 10.04842673892965 \times 10^{19}$ .

This augmentation in MPP peak amplitude is the signature of the presence of the defect. This augmentation is caused by the progress of the peeling in the tooth N° 15/16 (Table 1).

On the 12th day, the evolution of the crack is in the whole of the entire width of tooth N° 15/16, and the MPP peak amplitude reaches the value of  $MPP(1500, 25) = 80.54631341778420 \times 10^{19}$ .

Therefore, the autocorrelation function of the AMWT scalograms can detect early the defect.

#### 4 CONCLUSION

In this paper, we have presented a contribution in the field of early diagnosis of gear systems to detect the defects in gear systems in the early stage. This contribution is a new approach to the early defect

detection of gear systems. This approach is based on vibration analysis by the application of the AMWT. To prove the efficiency of this approach, simulation validation is given in the first part. Then, in the second part, the validation is done on a real system.

We have seen that the temporal and frequency representation cannot detect the defect in the early stage. However, the AMWT is an effective approach for detecting defects in gear reducers of the rotating machine.

In future work, we will investigate the proposed approach on a range of more representative data. Also, detecting the defect online is very suitable, and this aim will be the focalization of future work.

#### 5 ACKNOWLEDGEMENTS

This research was supported by Algerian Ministry of Higher Education and Scientific Research (PRFU N°: A10N01UN100120220001). The authors gratefully acknowledge the support of CETIM, which provided the vibration signals.

#### 6 REFERENCES

- [1] Panić, B., Klemenc, J., Nagode, M. (2020). Gaussian mixture model based classification revisited: application to the bearing fault classification. *Strojniški vestnik - Journal of Mechanical Engineering*, vol. 66, no. 4, p. 215-226, DOI:10.5545/sv-jme.2020.6563.
- [2] Pang, X., Cheng, B., Yang, Z., Li, F. (2019). A fault feature extraction method for a gearbox with a composite gear train based on EEMD and translation-invariant multiwavelet neighbouring coefficients. *Strojniški vestnik - Journal of Mechanical Engineering*, vol. 65, no. 1, p. 3-11, DOI:10.5545/sv-jme.2018.5441.
- [3] Do, V.T., Nguyen, L.C. (2016). Adaptive empirical mode decomposition for bearing fault detection. *Strojniški vestnik - Journal of Mechanical Engineering*, vol. 62, no. 5, p. 281-290, DOI:10.5545/sv-jme.2015.3079.
- [4] Ayad, M., Chikouche Dj., Boukezzoula, N., Rezki M. (2014). Search of a robust defect signature in gear systems across adaptive Morlet wavelet of vibration signals. *IET Signal Processing*, vol. 8, no. 9, p. 918-926, DOI:10.1049/iet-spr.2013.0439.
- [5] He, L., Hao, L., Qiao, W. (2021). Remote monitoring and diagnostics of pitch bearing defects in a MW-scale wind turbine using pitch symmetrical-component analysis. *IEEE Transactions on Industry Applications*, vol. 57, no. 4, p. 3252-3261, DOI:10.1109/TIA.2021.3079221.
- [6] Goyal, D., Dhami, S.S., Pabla, B.S. (2020). Non-contact fault diagnosis of bearings in machine learning environment. *IEEE Sensors Journal*, vol. 20, no. 9, p. 4816-4823, DOI:10.1109/JSEN.2020.2964633.
- [7] Etz, R., Petreus, D., Frentiu, T., Patarau, T., Orian, C. (2015). An indirect method and equipment for temperature monitoring

- and control. *Advances in Electrical and Computer Engineering*, vol. 15, no. 4, p. 87-95, DOI:10.4316/AECE.2015.04012.
- [8] de Oliveira A.K.V., Aghaei, M., Rütther, R. (2020). Aerial infrared thermography for low-cost and fast fault detection in utility-scale PV power plants. *Solar Energy*, vol. 211, p. 712-724. DOI:10.1016/j.solener.2020.09.066.
- [9] Sun, J., Wang, L., Li, J., Li, F., Li, J., Lu, H. (2021). Online oil debris monitoring of rotating machinery: A detailed review of more than three decades. *Mechanical Systems and Signal Processing*, vol. 149, art. ID 107341, DOI:10.1016/j.ymsp.2020.107341.
- [10] Sheng, S. (2016). Monitoring of wind turbine gearbox condition through oil and wear debris analysis: A full-scale testing perspective. *Tribology Transactions*, vol. 59, no. 1, p. 149-162, DOI:10.1080/10402004.2015.1055621.
- [11] Yao, J., Liu, C., Song, K., Zhang, X., Jiang, D. (2021). Fault detection of complex planetary gearbox using acoustic signals. *Measurement*, vol. 178, art. ID 109428, DOI:10.1016/j.measurement.2021.109428.
- [12] Glowacz, A. (2019). Fault detection of electric impact drills and coffee grinders using acoustic signals. *Sensors*, vol. 19, no. 2, p. 269, DOI:10.3390/s19020269.
- [13] Matic, D., Kanovic, Z. (2017). Vibration based broken bar detection in induction machine for low load conditions. *Advances in Electrical and Computer Engineering*, vol. 17, no. 1, p. 49-54, DOI:10.4316/AECE.2017.01007.
- [14] Xue, S., Howard, I. (2018). Torsional vibration signal analysis as a diagnostic tool for planetary gear fault detection. *Mechanical Systems and Signal Processing*, vol. 100, p. 706-728, DOI:10.1016/j.ymsp.2017.07.038.
- [15] Wang, S., Zhu, Z.K., He, Y., Huang, W. (2010). Adaptive parameter identification based on morlet wavelet and application in gearbox fault feature detection. *EURASIP Journal on Advances in Signal Processing*, vol. 2010, art. ID 842879, DOI:10.1155/2010/842879.
- [16] Daubechies, I. (1990). The wavelet Transform, time-frequency localisation and analysis. *IEEE Transactions on Information Theory*, vol. 36, no. 5, p. 961-1005, DOI:10.1109/18.57199.
- [17] Olkkonen, H., Olkkonen, J.T. (2010). Shift-invariant B-spline wavelet transform for multi-scale analysis of neuroelectric signals. *IET Signal Processing*, vol. 4, no. 6, p. 603-609. DOI:10.1049/iet-spr.2009.0109.
- [18] Al-Raheem, K.F., Roy, A., Ramachandran, K.P., Harrison, D.K., Grainger, S. (2009). Rolling element bearing faults diagnosis based on autocorrelation of optimized: wavelet de-noising technique. *The International Journal of Advanced Manufacturing Technology*, vol. 40, no. 3-4, p. 393-402, DOI:10.1007/s00170-007-1330-3.
- [19] Kankar, P.K., Sharma, S.C., Harsha, S.P. (2013). Fault diagnosis of rolling element bearing using cyclic autocorrelation and wavelet transform. *Neurocomputing*, vol. 110, p. 9-17, DOI:10.1016/j.neucom.2012.11.012.
- [20] McFadden, P.D. (1987). Examination of a technique for the early detection of failure in gears by signal processing of the time domain average of the meshing vibration. *Mechanical Systems and Signal Processing*, vol. 1, no. 2, p. 173-183, DOI:10.1016/0888-3270(87)90069-0.
- [21] Yin, J., Wang, W., Man, Z., Khoo, S. (2014). Statistical modeling of gear vibration signals and its application to detecting and diagnosing gear faults. *Information Sciences*, vol. 259, p. 295-303, DOI:10.1016/j.ins.2013.03.029.
- [22] Qin, Y., Mao, Y., Tang, B. (2013). Vibration signal component separation by iteratively using basis pursuit and its application in mechanical fault detection. *Journal of Sound and Vibration*, vol. 332, no. 20, p. 5217-5235, DOI:10.1016/j.jsv.2013.04.021.
- [23] Man, Z., Wang, W., Khoo, S., Yin, J. (2012). Optimal sinusoidal modelling of gear mesh vibration signals for gear diagnosis and prognosis. *Mechanical Systems and Signal Processing*, vol. 33, p. 256-274, DOI:10.1016/j.ymsp.2012.07.004.
- [24] Antoni, J., Randall, R.B. (2006). The spectral kurtosis: application to the vibration surveillance and diagnostics of rotating machines. *Mechanical Systems and Signal Processing*, vol. 20, no. 2, p. 308-331, DOI:10.1016/j.ymsp.2004.09.002.
- [25] Ayad, M., Kebir, A., Rezki, M., Saoudi, K., Benziane, M., Arabi, A. (2019). Early fault detection of gear system based on Wavelet Packets Transform. *1st International Conference on Sustainable Renewable Energy Systems and Applications*, p. 1-6, DOI:10.1109/ICSRESA49121.2019.9182269.